A Complete Charge Based Compact Model for Silicon Nanowire FETs Including Doping and Advanced Physical Effects

Feng Liu[1, 2], Jin He[1, 2*], Lining Zhang[2], Jian Zhang[2], Jinhua Hu[2], Xing Zhang[1, 2], and Mansun Chan[3]

[1]The Key Laboratory of Integrated Microsystems
Peking University Shenzhen Graduate School
Shenzhen, P. R. China

[2]TSRC, Institution of Microelectronics, EECS, Peking University
Beijing, P. R. China

[3]Dept. of Electronic and Computer Engineering
The Hong Kong University of Science & Technology
Hong Kong, P. R. China

*E-mail: frankhe@pku.edu.cn

***Abstract*-A charge-based silicon nanowire FET (SNWT) compact model has been developed. For the first time, inversion charge of SNWT with arbitrary doping concentration is described by an accurate equation including the effects of doping and volume inversion. Analytic drain current, transconductance, output conductance, terminal charges and capacitance are all physically derived and compared with numerical simulation. It shows that the core model is valid for all operation regions and a wide range of physical configuration including channel doping concentrations and geometrical dimensions. Moreover, advanced physical effects have been included in the model self-consistently.**

Keywords-nanowire; FET; compact model; doping; advanced physical effect

I. INTRODUCTION

In order to extend the silicon-based CMOS technology to and beyond the end of the International Technology Roadmap for Semiconductors (ITRS), the silicon nanowire transistor (SNWT) with surrounding-gate (SRG) architecture was proposed to achieve higher speed and lower power performance [1]. Though the channel may be designed with different doping concentrations, the previous developed compact models for SRG MOSFETs are only valid for undoped and heavily doped cases [2-3]. A general model for SNWTs valid for different doping concentrations is in urgent demand for circuit design. In this paper, a compact model for silicon nanowire transistors (SNWTs), available for a large range of doping concentrations (*i.e.* from 10^{10} to $10^{19} cm^{-3}$) and practical geometry sizes, is presented. Starting from Poisson's equation in the cylindrical coordinate system, an inversion charge (Q_{in}) equation is obtained for long channel SNWTs with arbitrary doping bodies. Then a charge based drain current (I_{ds}) expression is derived. Transconductance (g_m), output conductance (g_{ds}), terminal charges (Q) and capacitance coefficients (C_{ij}) are also obtained analytically and verified against TCAD data [4]. Moreover, advanced physical effects such as short channel effects (SCEs), quantum mechanical effects (QMEs) and high field mobility degradation, are also incorporated into this model.

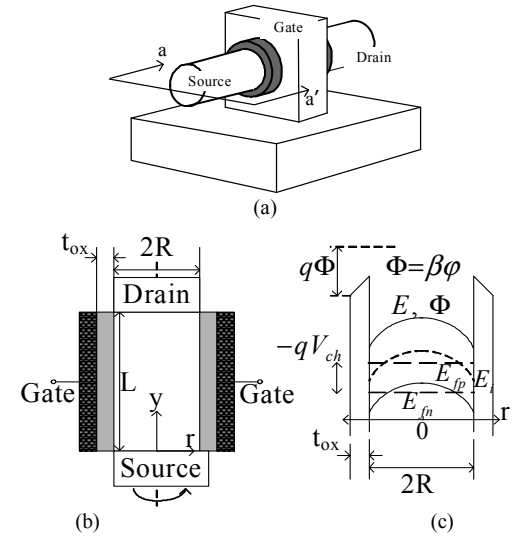

Figure 1. (a) Stereoscopic schematic, (b) cross-section schematic, and (c) energy band diagram of an *N*-type SNWT. t_{ox}=2nm, R=10nm, L=1μm and metal gate with mid-gap work-function is used unless specified in all comparisons with TCAD.

II. CORE MODEL FORMATION

A. Physical inversion charge equation

The device structure, coordinate system, and corresponding energy band diagram of a doped SNWT are shown in Fig.1. For an n-type device, the hole Fermi level E_{fp} is defined as the energy reference level. The 3D Poisson equation in the SNWT structure is written as

$$\frac{1}{r}\frac{d}{dr}\left(r\frac{d\phi}{dr}\right)+\frac{d^2\phi}{dy^2}=\frac{1}{L_D^{\,2}}\left[1+e^{\phi-v_{ch}-2\phi_f}\right] \qquad (1)$$

where $\phi_f=\ln\left(N_a/n_i\right)$ is the Fermi-potential, and $L_D^{\,2}=kT\varepsilon_{si}/q^2N_a$ is the Debye's length of the body with doping N_a. All other variables have their usual meanings, and all potentials are normalized by thermal voltage β, and the charges by β/C_{ox} where $C_{ox}=\varepsilon_{ox}/\left[R\ln\left(1+t_{ox}/R\right)\right]$ is the

This work is subsidized by the special funds for major state basic research project (973) and the National natural Science Funds of China (90607017). This work is also partially supported by a NEDO grant from Japan and an Earmarked Grant form the Research Grant Council of Hong Kong under the contract number 611207.

978-1-4244-1753-7/08/$25.00 ©2008 IEEE

effective oxide capacitance per gate area. The boundary conditions of (1) are

$$C_{ox}\left(v_{gs}-\Delta\phi-\phi_s\right)=\varepsilon_{si}\,d\phi/dr\big|_{r=R} \tag{2a}$$

$$\phi\left(r,y=0\right)=v_{bi}\ \text{and}\ \phi\left(r,y=L\right)=v_{bi}+v_{ds} \tag{2b}$$

This 3D problem is simplified into two separate parts along the vertical and current flow directions. Multiplying both sides of the 2D Poisson equation by r, and integrating once from r to r=0 gives

$$\frac{d\phi}{dr}=\frac{1}{L_D{}^2 r}\int_0^r\left[1+\mathrm{e}^{\phi-V_{ch}-2\phi_f}\right]rdr \tag{3}$$

In the weak inversion region, estimating the mobile charge density in the channel by its value n_0 at the centre of the film [5] gives a rough approximation of (3), and thus, the total mobile charge sheet density in the channel is given by $q_{in}=q^2n_0R/2kTC_{ox}$. Then, (3) becomes

$$d\phi=\frac{C_{ox}}{\varepsilon_{si}R}\left(q_{dep}+q_{in}\right)rdr \tag{4}$$

where $q_{dep}=q^2N_aR/2kTC_{ox}$ is the fixed charge density in the channel. Substituting (4) in (3) and considering (2a) yield [6]:

$$v_{gs}-v_{th0}-\Delta v_{th,VOL}-v_{ch}=q_{in}+\ln q_{in}+\ln\left(1+H\cdot q_{in}\right) \tag{5}$$

where $v_{th0}=\Delta\phi+2\phi_f+q_{dep}-\ln 4\varepsilon_{si}q_{dep}/RC_{ox}$ is the threshold voltage (V_{th}) similarly to the bulk MOSFET; $\Delta v_{th,VOL}=-\ln\left(1-\exp\left(-C_{ox}Rq_{dep}/2\varepsilon_{si}\right)\right)/2q_{dep}$ is the extra part of threshold voltage induced by the special geometric structure of SNWT. $v_{th}=v_{th0}+\Delta v_{th,VOL}$ is the total threshold voltage, and its verification is shown in Fig. 2. The transistor volume inversion effect is reflected by the H-factor in the third term of the RHS of (5). The H-factor can be obtained by analyzed the transistor behavior in the strong inversion region [6]:

$$H=\exp\left(-\Delta v_{th,VOL}\right) \tag{6}$$

With the physical modeling of v_{th} and H, charge control equation (5) can be applied in all operation regions, from weak to strong inversion and from intrinsic to heavy doping concentrations. To verify (5), the corresponding numerical results are obtained from the Sentaurus tools [4]. Fig. 3(a) illustrates the model predicted Q_{in} versus V_{gs} curves with different N_a, compared with the 3-D simulation results. Fig.3 (b) and (c) compared the model predicted Q_{in} versus V_{gs} curves for both intrinsic and heavily-doped SNWTs with

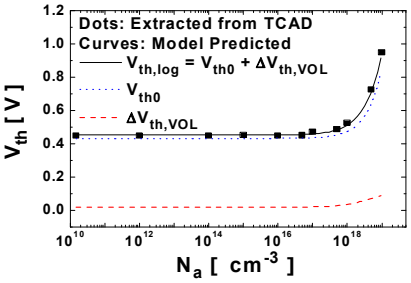

Figure 2. V_{th} model is compared with TCAD extracted by second derivative method in a long channel SNWT. V_{th0} and $\Delta V_{th,VOL}$ are its two contributions.

R variation against the numerical simulation, respectively. Excellent matching between the proposed model and numerical simulation can be observed, from intrinsic to 5×10^{18}cm^{-3} or heavier N_a until partial-depletion occurs.

B. Drain current, transconductance, terminal charges and capacitance coefficients

Starting from (5), the drain current model can be developed from the well-known Pao-Sah's dual integral [7]:

$$I_{ds}=\frac{\mu_{eff}\left(2\pi R\right)}{L_{eff}}\frac{C_{ox}}{\beta^2}\int_{q_s}^{q_d}q_{in}\frac{dv_{ch}}{dq_{in}}dq_{in} \tag{7}$$

where μ_{eff} is the effective mobility; q_d and q_s are normalized inversion charge per unit gate area at the source and drain terminals. After getting dv_{ch}/dq_{in} in terms of inversion charge from (5), the integration result of (7) gives the analytical drain current expression as:

$$I_{ds}=\frac{2\pi R\mu_{eff}C_{ox}}{\beta^2L_{eff}}\left[f\left(q_d\right)-f\left(q_s\right)\right] \tag{8}$$

with $f\left(q_{in}\right)=-q_{in}{}^2/2-2q_{in}+H^{-1}\ln\left(1+H\cdot q_{in}\right)$.

Transconductance and output conductance can be derived analytically from the expressions of drain current:

$$g_m=\partial I_{ds}/\partial V_{gs}\big|_{V_{ds}}=2\pi R\mu_{eff}C_{ox}\left(q_s-q_d\right)/\beta L_{eff} \tag{9a}$$

$$g_{ds}=\partial I_{ds}/\partial V_{ds}\big|_{V_{gs}}=2\pi R\mu_{eff}C_{ox}q_d/\beta L_{eff} \tag{9b}$$

Analytical expressions for terminal charge are desired for transient circuit simulation. For a SNWT, there are three terminal charges, associating with gate, drain, and, source denoted as Q_g, Q_d and Q_s, respectively. They can be estimated

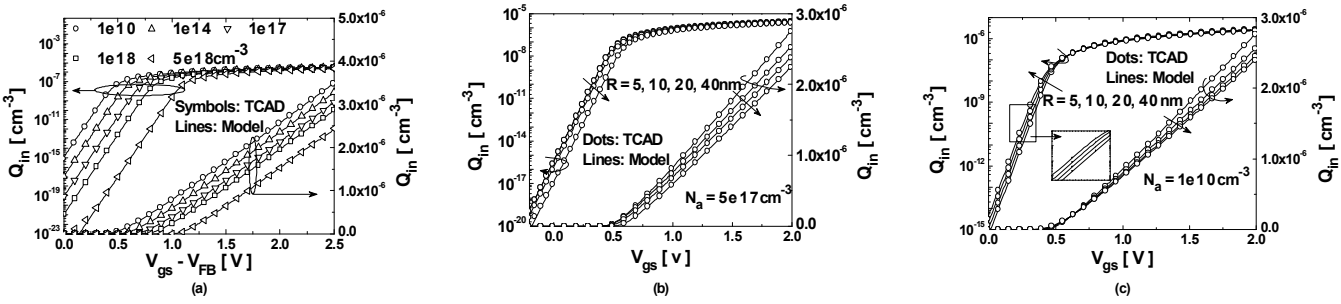

Figure 3. Inversion charge equation verification for long channel SNWTs (a) with doping variation, (b) with geometric size variation in doped case and (c) with geometric size variation in undoped case (volume inversion effect in lightly doped SNWT is illustrated in the inset of (c)).

by using the Ward-Dutton linear-charge-partition method:

$$Q_g = 2\pi RC_{ox}\beta^{-2}\int_0^{V_{ds}} q_{in}dy \tag{10a}$$

$$Q_d = -2\pi RC_{ox}\beta^{-2}\int_0^{V_{ds}} \frac{y}{L} q_{in}dy \tag{10b}$$

$$Q_s = -Q_g - Q_d \tag{10c}$$

where y/L are obtained from the current continuity condition

$$y/L = \left[f(q_{in}) - f(q_s)\right] / \left[f(q_d) - f(q_s)\right] \tag{11}$$

Again, current continuity condition need be used to obtain the analytical terminal charges (10).

The intrinsic capacitances network of SNWT as a three-terminal device contains nine components. The expressions for these capacitances are determined by following matrix

$$\begin{bmatrix} C_{gg} & -C_{gd} & -C_{gs} \\ -C_{dg} & C_{dd} & -C_{ds} \\ -C_{sg} & -C_{sd} & C_{ss} \end{bmatrix} \begin{bmatrix} \delta V_g \\ \delta V_d \\ \delta V_s \end{bmatrix} = \begin{bmatrix} \delta Q_g \\ \delta Q_d \\ \delta Q_s \end{bmatrix} \tag{12}$$

By this definition and the chain rule, four independent capacitances can be derived analytically through the inversion charge at the source and drain terminals [8]. We did not list the analytical results of the terminal charges and capacitances due to the length limit of the paper.

The model predicted I-V characteristics are verified by comparing with results from Sentaurus under various bias voltages, a wide range of doping concentrations and geometric dimensions as shown in Fig.4. The error between the proposed model and numerical simulation is less than 5% for devices from intrinsic to heavily doped body ($10^{19}cm^{-3}$).

In contrast to digital circuits, analog design focus on the first derivatives such as g_m/I_{ds} and C_{ij}, which are shown in Fig.5. At V_{ds}=0, C_{gs}=C_{gd} and C_{sg}=C_{dg} in the figures indicate that the developed model has inherent source/drain symmetry characteristic, which is important for analog and RF applications. Note that the verifications of the core I-V and C-V models are done without any fitting parameters.

III. ADVANCED PHYSICAL EFFECTS

A. Modeling short channel effects (SCE)

In generally, SCEs induce V_{th} roll-off, subthreshold slope (SS) degradation, DIBL, *et al.*. In addition, channel length modulation and carrier velocity saturation and overshoot becomes important at short channel length as well. In this work, SCEs are modeled following the BSIM5 approach [9]. An inversion charge solution can be obtained using (2b):

$$\frac{v_{gs} - v_{th} - \alpha \cdot v_{ch}}{\alpha} = \frac{q_{in}}{\alpha} + \ln q_{in} + \ln\left(1 + H \cdot q_{in}\right) \tag{13}$$

where $\alpha = 1 + 2 \cdot f_{SCE}$ is related to SS;

$f_{SCE} = 1/\left[2\cosh\left(L/2/\lambda\right) - 2\right]$ is the SCEs factor;

$v_{th} = v_{th0} + \Delta v_{th,VOL} + \Delta v_{th,SCE}$ is the new threshold voltage;

$\Delta v_{th,SCE} = f_{SCE} \cdot \left[2 \cdot \left(v_{th,Long} - q_{dep} - v_{bi}\right) - v_{ds}\right]$ is the threshold voltage roll-off induced by the SCEs.

$\lambda = \sqrt{t_{oxeff} R\varepsilon_{si} / 2\varepsilon_{ox} + R^2/4}$ is the natural length of SNWT by assuming the leakage path lies at the center of the channel [3].

Drain current expression can then be derived using (13):

$$I_{ds} = 2\pi R\mu_{eff} C_{oxeff} \beta^{-2} L_{eff}^{-1} \left[f(q_d) - f(q_s)\right] \tag{14}$$

with $f(q_{in}) = -q_{in}^2/2\alpha - 2q_{in} + H^{-1}\ln\left(1 + H \cdot q_{in}\right)$.

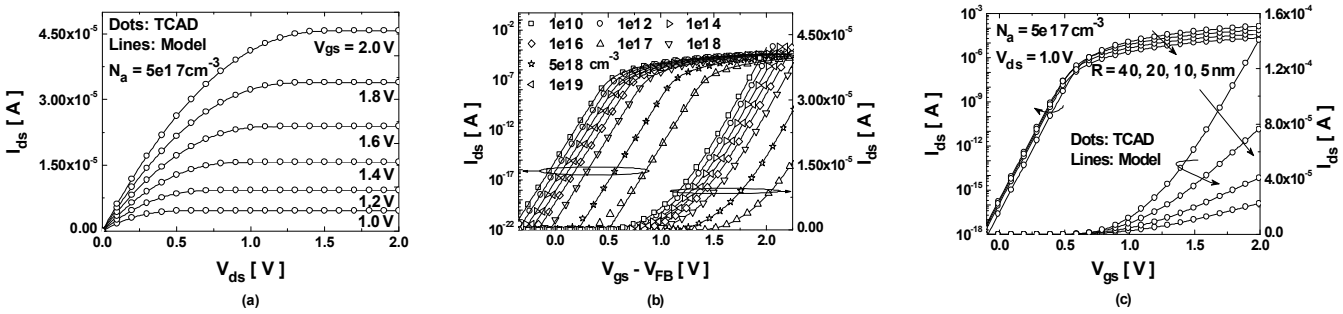

Figure 4. *dc* I-V characteristics verification for long channel SNWTs (a) I_{ds}-V_{ds} (b) I_{ds}-V_{gs} with doping variation and (c) I_{ds}-V_{gs} with geometric size variation.

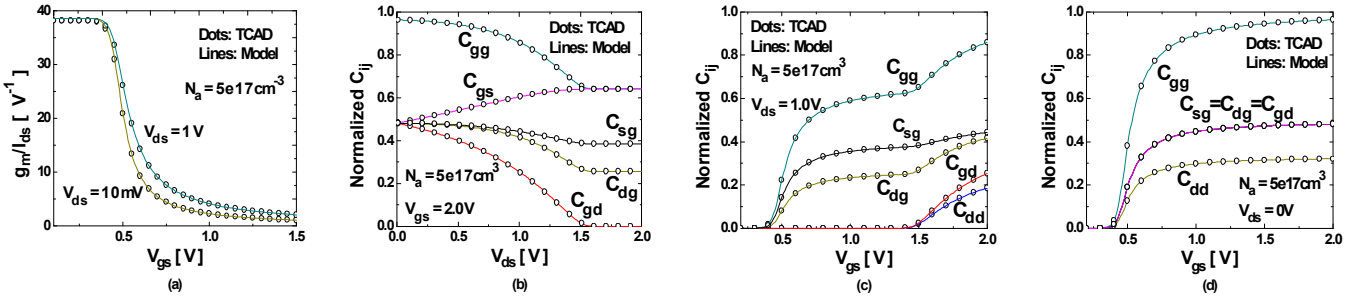

Figure 5. *ac* characteristics verification of the model for a long channel SNWT. (a) g_m-efficiency, (b) *C*-V_{ds}, (c) *C*-V_{gs} (at V_{ds}≠0) and (d) *C*-V_{gs} (at V_{ds}=0). Model symmetry characteristic can be observed at V_{ds}=0, illustrating its applicability for analog circuit design.

Comparison with numerical simulation in Fig.6(a) shows the correctness of the threshold voltage roll-off and DIBL described by the proposed SCEs model. Fig.6 (b) shows that the transfer characteristics with SS degradation as predicted in the proposed the short channel model. Velocity saturation, velocity overshoot and ballistic transport (source-end velocity limit) is handled in a unified way using the saturation charge concept [9]:

$$q_{ssat(dsat)} = \frac{q_{d(s)}}{1+2\beta n v_{sat} L_{eff} \big/ \mu_{eff} \left(2n + k_{sativ} q_{d(s)}\right)} \tag{15a}$$

$$q_{ineff} = \sqrt[m]{q_{insat}{}^{m} + q_{in}{}^{m}} \tag{15b}$$

where n and m are the only parameters. A complete ballistic transport model is not considered in this work, as ballistic transport will not be significant until the channel length is scaled to less than 10nm [3].

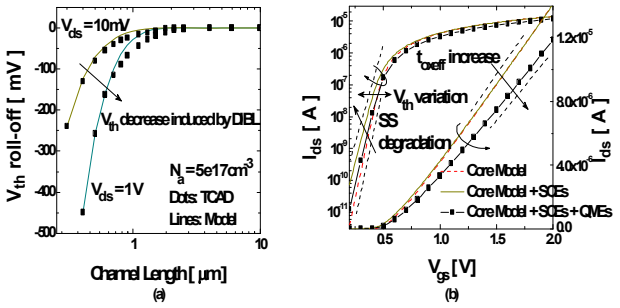

Figure 6. Advanced physical effects modeling for a small size SNWT (a) V_{th} roll-off and DIBL induced by SCEs are modeled and (b) SS degradation induced by SCEs and t_{oxeff} increase by QMEs are modeled.

B. Modeling quantum-mechanical (QM) effects and other advanced physical effects

In highly scaled device, the QM confinement of the carrier in the thin silicon channel is significant. There are two kinds of QM effects can affect the behavior of the transistor. One is the deviation of the location of peak carrier concentration from the surface under the strong field, and can be modeled by a decrease in the gate capacitance [10]:

$$\Delta t_{ox} = \Delta = a \cdot \left(\hbar^2 \big/ 2qm_e E_{avg}\right)^{1/3} \tag{16a}$$

$$C_{oxeff} = \varepsilon_{ox} \left[(R - \Delta/3) \cdot \ln\left((R + t_{ox}) \big/ (R - \Delta/3) \right) \right]^{-1} \tag{16b}$$

where m_e is the effective mass of the electron, and $E_{avg} = C_{ox}\left(q_{dep} + \bar{q}_{in}/3\right)\big/\beta\varepsilon_{si}$ is the average surface field. In addition, there is a strong carrier confinement in nanoscale potential well even at low electric fields in the channel. The corresponding reduction of the amount of carriers can be modeled by widening the effective band-gap [11] and replace v_{ch} in (13) by

$$v_{ch} \to v_{ch} + E_0/q = v_{ch} + \lambda_q \left(\hbar^2 \pi^2 / 4qm_e R^2\right) \tag{17}$$

The simulation results shown in Fig.6(b) illustrates the model can predicted the threshold voltage roll off and gate capacitance degradation induced by QME correctly. Other advanced physical effects modeling such as poly-depletion effects and mobility degradation are imported from the BSIM5 approach. The *dc* characteristics for a small size SNWT predicted by the complete compact model is demonstrated in Fig.7.

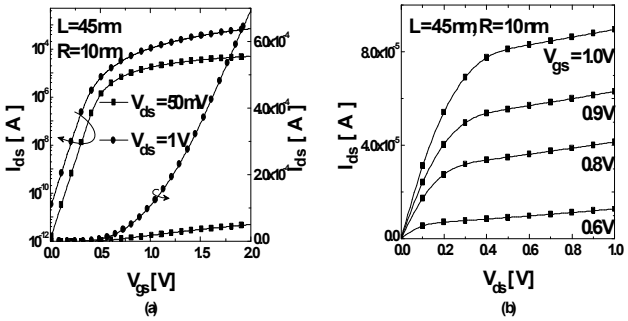

Figure 7. (a) I_{ds}-V_{gs} and (b) I_{ds}-V_{ds} characteristics predicted by the complete compact model for a small size SNWT.

V. CONCLUSIONS

In summary, we present a compact model for silicon nanowire transistors in terms of inversion charge at the source and drain terminals. The comparison with TCAD indicates that the core I-V and C-V models are accurate for a wide range of biasing, doping concentrations and geometrical dimensions. Advanced physical effects such as SCEs and QMEs in small size nanowire transistors are also included in the model in a self-consistent way.

REFERENCES

[1] Y. Cui, Z. Zhong, D. Wang, W. Wang, and C. M. Lieber, "High performance silicon nanowire field effect transistors," *Nano Lett.*, vol. 3, no. 2, pp. 149–152, Feb. 2003.

[2] D. Jiménez, *et al.*, "Continuous analytic current-voltage model for surrounding gate MOSFETs," IEEE Electron Device Lett., vol. 25, no. 8, pp. 571–573, Aug. 2004.

[3] C. P. Auth, and J. D. Plummer, "Scaling theory for cylindrical, fully-depleted, surrounding-gate MOSFETs," IEEE Electron Device Lett., vol. 18, no. 2, pp. 74–76, Feb. 1997.

[4] *TCAD Sentaurus Device User's Manual*, Synopsys, Mountain View, CA, 2005.

[5] P. Francis, A. Terao, D. Flandre, and F. Van de Wiele, "Characteristics of nMOS/GAA (Gate-All-Around) transistors near threshold," Microelectronic Engineering, vol. 19, no. 1-4, pp. 815-818, Sept. 1992.

[6] F. Liu, J. He, *et al.*, "A charge-based model for long-channel cylindrical surrounding-gate MOSFETs from intrinsic channel to heavily doped body," to be appeared in IEEE Trans. Electron Devices, Aug. 2008.

[7] H. C. Pao and C. T. Sah, "Effects of diffusion current on characteristics of metal-oxide (insulator)-semiconductor transistors," Solid-State Electron., vol. 9, no. 6, pp. 927-937, Jun. 1966.

[8] O. Moldovan, B. Iñiguez, D. Jiménez, and J. Roig, "Analytical charge and capacitance models of undoped cylindrical surrounding-gate MOSFETs," IEEE Trans. Electron Devices, vol. 54, no. 1, pp. 162-165, Jan. 2007.

[9] J. He, X. Xi, H. Wan, M. Dunga, M. Chan, and A. M. Niknejad, " BSIM5: An advanced charge-based MOSFET model for nanoscale VLSI circuit simulation," Solid-State Electronics, vol. 51, no. 3, pp. 433–444, Mar. 2007.

[10] J. H. Davies, The physics of low-dimensional semiconductors, Cambridge University Press, 1998.

[11] R. Rios, N. D. Arora, C.-L. Huang, N. Khabil, J. Faricelli, and L. Gruber, "A physical compact MOSFET model, including quantum mechanicals effects, for statistical circuit design applications," in *IEDM Tech. Dig.*, 1995, pp. 947–950.